INTERNATIONAL JOURNAL FOR NUMERICAL AND ANALYTICAL METHODS IN GEOMECHANICS
Int. J. Numer. Anal. Meth. Geomech., **24**, 47–71 (2000)

NUMERICAL MODELLING OF COMPETITIVE COMPONENTS TRANSPORT WITH NON-LINEAR ADSORPTION

DAICHAO SHENG* AND DAVID W. SMITH

Department of Civil, Surveying and Environmental Engineering, The University of Newcastle, NSW 2308, Australia

SUMMARY

A characteristic finite element (CFE) algorithm for modelling contaminant transport problems coupled with non-linear competitive adsorption is presented. An alternative algorithm, termed as the transport-equilibrium Petrov–Galerkin (TEPG) methods in this paper, is also presented for comparison. Through analyses of a number of examples with Peclet number ranging from zero to infinity, it is shown that the CFE algorithm is very competitive with the middle–point TEPG method in terms of accuracy, stability and efficiency. The fully explicit and fully implicit TEPG methods are found to be less appropriate for transport problems coupled with non-linear equilibrium equations. Copyright © 2000 John Wiley & Sons, Ltd.

KEY WORDS: contaminant transport; competitive adsorption; finite element algorithms

INTRODUCTION

When modelling of transient contaminant transport in soils, the governing advection–dispersion equations are commonly assumed to be linear (i.e. with coefficients independent of the unknown concentration[1]). One of the requirements for this linearity is the use of a linear adsorption isotherm. However, it is well known that the adsorption of contaminants onto the soil particles is more appropriately described by non-linear adsorption isotherms. This is not only because the total adsorption capacity of the soil is limited, but also because different components have different affinities for the soil and these components can compete for the limited adsorption sites.[2,3]

Introducing a non-linear adsorption isotherm to an advection–dispersion equation immediately alters the behaviours of the transport process. While a contaminant subject to linear adsorption transports with a uniformly retarded velocity,[1] the contaminant subject to non-linear adsorption has a tendency to form concentration shock and rarefaction waves. In deriving their analytical solutions, Sheng and Smith[4] demonstrated how different the solution of a non-linear advection problem can be from that of a linear advection problem. In the example they gave, the concentration front velocity computed using an approximate initial tangent linear adsorption isotherm is only 13 per cent of that computed using a more accurate non-linear adsorption isotherm.

* Correspondence to: Dr. Daichao Sheng, Department of Civil, Surveying and Environmental Engineering, University of Newcastle, NSW 2308, Australia, E-mail: daico@civeng.newcastle.edu.au

CCC 0363–9061/2000/010047–25$17.50

Received 4 December 1998
Revised 11 March 1999

Introducing a non-linear competitive adsorption isotherm to the transport equations for miscible components eventually leads to a set of coupled non-linear partial differential equations which need to be solved simultaneously for all competing components. Effective solution techniques for such equation systems are limited. Yeh and Tripathi[5] gave a critical review on possible solution strategies for linear transport equations coupled with non-linear equilibrium equations and pointed out that the only practical strategy is the so-called 'sequential iteration approach'.

In this paper, the characteristic finite element method, presented by Sheng and Axelsson for general coupled flow problems,[6] will be modified and used to solve the advection–dispersion problem coupled with non-linear competitive adsorption equations. A Petrov–Galerkin finite element method, incorporated into the sequential iteration approach recommended by Yeh and Tripathi,[5] will also be described in detail and used for comparison. For simplicity, both the methods will be described in one spatial dimension. For a constant fluid velocity, as used in this paper, the extension of these methods to multidimensional space is straightforward. With one of the space co-ordinates defined in the same direction of the fluid velocity, we need only to include the diffusion terms in other directions. However, for a non-linear fluid velocity, more research is required to extend these methods to multidimensional space.

TRANSPORT OF MISCIBLE COMPONENTS SUBJECT TO COMPETITIVE ADSORPTION

The adsorption of competitive components in a soil is usually described by the multi-component Langmuir–type isotherm (see e.g. Reference 7),

$$S_i = \frac{K_i C_i Q}{1 + \sum_{j=1}^{\mathrm{Nos}} K_j C_j}, \quad i = 1, 2, \ldots, \mathrm{Nos} \tag{1}$$

where C is the concentration in the soil pore liquid, S is the concentration adsorbed on the soil particle surfaces, K is an adsorption parameter, Q is the maximum adsorption capacity of the soil, the subscript i and j refer to the ith and jth component respectively, and Nos is the total number of components.

It is clear from equation (1) that the Langmuir adsorption isotherm reduces to a linear adsorption isotherm only if the sum $\sum_{j=1}^{\mathrm{Nos}} K_j C_j$ is significantly less than one. In this case, the adsorbed concentration depends only on the pore fluid concentration of the same component, and the product $K_i Q$ is equivalent to the distribution factor K_d.[1] If the sum $\sum_{j=1}^{\mathrm{Nos}} K_j C_j$ is significantly larger than 1, the total adsorbed concentration for all components approaches the maximum adsorption capacity Q, i.e. $\sum_{j=1}^{\mathrm{Nos}} S_j \approx Q$. In general, the relative dominance of component i is measured by the ratio of the product $K_i C_i$ to the sum $\sum_{j=1}^{\mathrm{Nos}} K_j C_j$.

Equation (1) can also be used to describe chemical processes like ion exchange.[8,9] In certain cases additional equilibrium equations need to be satisfied, which in general reduce the number of dependent equations. This paper, however, will only deal with the reversible equilibrium process described by (1). The equilibrium between liquid concentration C and adsorbed concentration S is assumed to be invariably instantaneous.

The advection–dispersion equation for the transport of miscible components through a soil, can be written as[10]

$$\frac{\partial C_i}{\partial t} + \frac{\rho_\mathrm{d}}{n}\frac{\partial S_i}{\partial t} = D_i \frac{\partial^2 C_i}{\partial x^2} - \frac{v}{n}\frac{\partial C_i}{\partial x} - E_i, \quad i = 1, 2, \ldots, \mathrm{Nos}. \tag{2}$$

where D_i is the hydrodynamic dispersion coefficient, v is the Darcian fluid velocity, ρ_d is the dry density of the soil, n is the volumetric water content or the porosity for a saturated soil, E_i is a general source/sink term for component i, t is the time and x is the space co-ordinate. As hydrodynamic dispersion is modelled by the Fick law in equation (2), it will generally be referred to as diffusion in this paper.

Differentiating S_i with respect to t according to the chain rule gives

$$\frac{\partial S_i}{\partial t} = \sum_{j=1}^{\text{Nos}} \frac{\partial S_i}{\partial C_j} \frac{\partial C_j}{\partial t}, \quad i = 1, 2, \ldots, \text{Nos} \tag{3}$$

where the derivative $\partial S_i / \partial C_j$ is obtained by differentiating equation (1) and it obviously depends on solution concentration C_j of each component.

Substituting equation (3) into equation (2) leads to

$$\frac{\partial C_i}{\partial t} + \frac{\rho_d}{n} \sum_{j=1}^{\text{Nos}} \left(\frac{\partial S_i}{\partial C_j} \frac{\partial C_j}{\partial t} \right) = D_i \frac{\partial^2 C_i}{\partial x^2} - \frac{v}{n} \frac{\partial C_i}{\partial x} - E_i, \quad i = 1, 2 \ldots, \text{Nos} \tag{4}$$

From equation (4), it can be seen that the governing equation for any component, i, is coupled to the concentrations of other components through the term $\partial S_i / \partial C_j$. This means that the governing equations for transport of competitive components are a set of coupled partial differential equations that have to be solved simultaneously for all components.

Now let A_{ij} be defined as

$$A_{ij} = \begin{cases} 1 + \dfrac{\rho_d}{n} \dfrac{\partial S_i}{\partial C_i}, & i = j \\ \dfrac{\rho_d}{n} \dfrac{\partial S_i}{\partial C_j}, & i \neq j \end{cases} \tag{5}$$

the governing equations for all components can then be written in a matrix form as

$$\mathbf{A} \frac{\partial \mathbf{C}}{\partial t} = \mathbf{D} \frac{\partial^2 \mathbf{C}}{\partial x^2} - \mathbf{V} \frac{\partial \mathbf{C}}{\partial x} - \mathbf{E} \tag{6}$$

where

$$\mathbf{C} = \{C_1, C_2, C_3, \ldots\}^{\mathrm{T}}$$

$$D_{ij} = \begin{cases} D_i, & i = j \\ 0 & i \neq j \end{cases}$$

$$V_{ij} = \begin{cases} \dfrac{v}{n}, & i = j \\ 0 & i \neq j \end{cases}$$

$$E_{ij} = \begin{cases} E_i, & i = j \\ 0 & i \neq j \end{cases}$$

Common initial and boundary conditions associated with the transport equation (6) can be written as

$$\mathbf{C} = \mathbf{C}^0(x), \quad t = 0 \tag{7}$$

$$\mathbf{C} = \mathbf{G}(t), \quad x = \Gamma_1 \tag{8}$$

$$-D\frac{\partial \mathbf{C}}{\partial x} = \mathbf{Q}(t), \quad x = \Gamma_2 \tag{9}$$

There are two major difficulties in solving the problem defined by equations (6)–(9). The first one is due to the presence of both the first- and second-order spatial derivatives in equation (6). It is known that standard numerical methods, such as the Galerkin finite element method or the central finite difference method, have problems in obtaining accurate and stable solutions for advection-dominated transport. Advanced numerical techniques for solving an independent advection–diffusion equation have been addressed in the literature.[11] The second difficulty in solving equation (6) is due to the non-linear coupling between different components. Though matrices **D**, **V** and **E** are diagonal and usually independent of the unknown C_i, the matrix **A** does in general have off-diagonal terms that are dependent on the unknown concentrations.

CHARACTERISTIC FINITE ELEMENT METHOD

The governing equation (6) can be rewritten in a Lagrangian form as

$$\mathbf{A}\frac{\mathrm{D}\mathbf{C}}{\mathrm{D}t} = \mathbf{D}\frac{\partial^2 \mathbf{C}}{\partial x^2} = \mathbf{E} \tag{10}$$

where

$$\frac{\mathrm{D}\mathbf{C}}{\mathrm{D}t} = \frac{\partial \mathbf{C}}{\partial t} + \mathbf{A}^{-1}\mathbf{V}\frac{\partial \mathbf{C}}{\partial x} \tag{11}$$

denotes the material derivative.

Now introduce a new unknown vector, $\tilde{\mathbf{C}}$, and let it satisfy the following initial value problem,

$$\mathbf{A}\frac{\mathrm{D}\tilde{\mathbf{C}}}{\mathrm{D}t} = \mathbf{A}\frac{\partial \tilde{\mathbf{C}}}{\partial t} + \mathbf{V}\frac{\partial \tilde{\mathbf{C}}}{\partial x} = \mathbf{0} \tag{12}$$

$$\tilde{\mathbf{C}}(x, 0) = \mathbf{C}(x, 0) = \mathbf{C}^0(x) \tag{13}$$

The system of hyperbolic equation (12) together with the initial condition (13) define a advection problem. Subtracting equation (12) from (10) gives the following diffusion equation:

$$\mathbf{A}\left(\frac{\mathrm{D}\mathbf{C}}{\mathrm{D}t} - \frac{\mathrm{D}\tilde{\mathbf{C}}}{\mathrm{D}t}\right) = \mathbf{D}\frac{\partial^2 \mathbf{C}}{\partial x^2} - \mathbf{E} \tag{14}$$

The appropriate initial condition for this diffusion equation is

$$\mathbf{C}(x, 0) = \tilde{\mathbf{C}}(x, 0) = \mathbf{C}^0(x) \tag{15}$$

The boundary conditions for the diffusion problem are defined by equations (8) and (9).

By means of the procedure above, the advection–diffusion problem defined by equations (6)–(9) is decomposed into an advection problem and a diffusion problem. The advection problem defined by equations (12) and (13) can be solved analytically if the system can be uncoupled into independent equations for each concentration C_i. The diffusion problem can be solved by a standard Galerkin finite element method. The advantage of this decomposition is that any advection–diffusion problem, no matter which transport mechanism is dominant, can be effectively solved. As a matter of fact, both pure advection and pure diffusion problems can be solved using the technique described below.

The analytical solution to the advection problem starts with the transformation

$$\tilde{\mathbf{C}} = \mathbf{P}\mathbf{U} \tag{16}$$

where $\mathbf{P}$ is the eigenvector matrix of $\mathbf{A}$ and $\mathbf{U}$ is the new unknown vector. Replacing $\tilde{\mathbf{C}}$ by $\mathbf{U}$ and multiplying equation (12) by $\mathbf{P}^{-1}$ from left lead to

$$\mathbf{P}^{-1}\mathbf{A}\mathbf{P}\frac{\partial \mathbf{U}}{\partial t} + \mathbf{P}^{-1}\mathbf{V}\mathbf{P}\frac{\partial \mathbf{U}}{\partial x} = \mathbf{0} \tag{17}$$

The multiplier $\mathbf{P}^{-1}\mathbf{A}\mathbf{P}$ in the first left term in the equation above becomes, by definition of $\mathbf{P}$, the diagonal matrix $\mathbf{\Gamma}$ with the eigenvalues of $\mathbf{A}$ on its diagonal. The multiplier $\mathbf{P}^{-1}\mathbf{V}\mathbf{P}$ in the second term remains as $\mathbf{V}$, since $\mathbf{V}$ is a homogeneous diagonal matrix. Therefore, we have

$$\mathbf{\Gamma}\frac{\partial \mathbf{U}}{\partial t} + \mathbf{V}\frac{\partial \mathbf{U}}{\partial x} = \mathbf{0} \tag{18}$$

This is an uncoupled system of hyperbolic equations that can be solved independently. The solution of each equation in (18) is simply the translation of its initial condition along its characteristic lines, i.e.

$$U_i = U_i^0\left(x - \frac{v}{n\lambda_i}t\right) = \sum_{j=1}^{\text{Nos}} \bar{P}_{ij}\bar{C}_j^0\left(x - \frac{v}{n\lambda_i}t\right) = \sum_{j=1}^{\text{Nos}} \bar{P}_{ij}C_j^0\left(x - \frac{v}{n\lambda_i}t\right) \tag{19}$$

where λ_i is the ith eigenvalue of $\mathbf{A}$, $\bar{P}_{ij}$ is the element in ith row and jth column of matrix $\mathbf{P}^{-1}$. Note that $\bar{P}_{ij}$ is computed at the location $x - (v/n\lambda_i)t$ where C_j^0 is taken. In a fixed domain $x_a \leqslant x \leqslant x_b$, equation (19) is only valid when

$$x_a \leqslant x - \frac{v}{n\lambda_i}t \leqslant x_b \tag{20}$$

Near the inflow boundary, $x - vt/n\lambda_i$ may lie outside the interval $[x_a, x_b]$ and the material particle is new in the domain. In this case, the concentration is determined by the inflow concentration

$$U_i = \sum_{j=1}^{\text{Nos}} \bar{P}_{ij}G_j = Z_i, \quad \left(x - \frac{vt}{n\lambda_i}\right) \notin [x_a, x_b] \tag{21}$$

Once $\mathbf{U}$ is known, the unknown $\tilde{\mathbf{C}}$ can be calculated from (16), i.e.

$$\tilde{\mathbf{C}}(x) = \mathbf{P}(x)\mathbf{U}(x) \tag{22}$$

where the matrices are written in functions of x to indicate the locations they are computed. For non-linear hyperbolic equation systems where $\mathbf{P}$ also varies with t, $\tilde{\mathbf{C}}$ has to be computed from $\mathbf{U}$ time step by time step.

The solution to the diffusion problem defined by equations (14), (15), (8) and (9) flows the standard Galerkin procedure. Using the discretization of the unknown $\mathbf{C}$ inside a Nod-noded element

$$\mathbf{C} = \sum_{j=1}^{\mathrm{Nos}} \mathbf{N}_j \underline{\mathbf{C}}_j = \mathbf{N}\underline{\mathbf{C}} \tag{23}$$

and applying the Galerkin weighting procedure to equation (14) lead to the following system of ordinary differential equations:

$$\mathbf{M}\left(\frac{\mathrm{D}\underline{\mathbf{C}}}{\mathrm{D}t} - \frac{\mathrm{D}\underline{\tilde{\mathbf{C}}}}{\mathrm{D}t}\right) + \mathbf{H}\underline{\mathbf{C}} + \mathbf{F} = \mathbf{0} \tag{24}$$

In equation (23), Nod is the number of nodes of the element, $\underline{\mathbf{C}}_j$ contains the values of $\mathbf{C}$ at node j, $\mathbf{N}_j$ is the shape function matrix for node j and $\mathbf{N}_j = N_j\mathbf{I}$ with N_j being the shape function and $\mathbf{I}$ being the identity matrix of dimension of Nos × Nos. In a system of Nos components, $\mathbf{N}$ is a Nos × (Nos × Nod) dimension matrix consisting of $\mathbf{N}_j$, and $\underline{\mathbf{C}}$ is a Nos × Nod dimension vector consisting of $\underline{\mathbf{C}}_j$. The number of components corresponds to the degrees of freedom at nodes. The matrices in equation (24) are given as follows;

$$\mathbf{M} = \sum \int_{\Omega^e} \mathbf{N}^{\mathrm{T}}\mathbf{A}\mathbf{N}\,\mathrm{d}x$$

$$\mathbf{H} = \sum \int_{\Omega^e} \frac{\partial \mathbf{N}^{\mathrm{T}}}{\partial x}\mathbf{D}\frac{\partial \mathbf{N}}{\partial x}\,\mathrm{d}x$$

$$\mathbf{F} = \sum \int_{\Omega^e} \mathbf{N}^{\mathrm{T}}\mathbf{E}\,\mathrm{d}x + (\mathbf{N}^{\mathrm{T}}\mathbf{Q})|_{x=\Gamma_2}$$

where the source terms $\mathbf{E}$ are assumed to be concentration independent. For concentration-dependent source terms such as the first-order decay kinetics, the $\mathbf{E}$ term goes to matrix $\mathbf{H}$ instead of vector $\mathbf{F}$.[6]

The time derivatives in the parentheses in equation (24) can be approximated by finite differences,

$$\frac{\mathrm{D}\underline{\mathbf{C}}}{\mathrm{D}t} = \frac{\underline{\mathbf{C}}^{k+1} - \underline{\mathbf{C}}^{k}}{\Delta t} \tag{25}$$

$$\frac{\mathrm{D}\underline{\tilde{\mathbf{C}}}}{\mathrm{D}t} = \frac{\underline{\tilde{\mathbf{C}}}^{k+1} - \underline{\mathbf{C}}^{k}}{\Delta t} \tag{26}$$

where $\underline{\mathbf{C}}^{k+1}$ is the unknown concentration vector at time level $t^{k+1} = t^k + \Delta t^k$, $\underline{\mathbf{C}}^k$ is the concentration vector at time level t^k, and $\underline{\tilde{\mathbf{C}}}^{k+1}$ is the concentration vector solved from the advection problem at time level $t^{k+1} = t^k + \Delta t^k$.

An effective time-stepping scheme for the ordinary differential equation system (24) is the explicit three-level scheme[12]

$$\mathbf{M}^k \left\{ \frac{\underline{\mathbf{C}}^{k+1} - \underline{\tilde{\mathbf{C}}}^{k+1}}{\Delta t} \right\} + \mathbf{H}^k \left\{ \frac{\mathbf{3}}{\mathbf{4}} \underline{\mathbf{C}}^{k+1} + \frac{\mathbf{1}}{\mathbf{4}} \underline{\tilde{\mathbf{C}}}^{k-1} \right\} + \mathbf{F}^{k+1} = \mathbf{0} \tag{27}$$

where $\underline{\tilde{\mathbf{C}}}^{k-1}$ is the concentration vector solved from the advection problem at time level $t^{k-1} = t^k - \Delta t^{k-1}$.

As mentioned earlier, the algorithm described above can be applied to solve purely advective or purely diffusive problems. For an advective problem, we need only to find the analytical solution of the problem defined by equations (12) and (13). For a diffusive problem, the first part for the analytical solution of the advection problem can be skipped. The algorithm for the characteristic finite element method can be summarized as follows:

1. At time step $t = t^k$, enter the time increment Δt^k at the current step and the time increment Δt^{k-1} at the previous step, the current concentration $\underline{\mathbf{C}}^k$, the concentration $\underline{\mathbf{C}}^{k-1}$ at the previous time step $t^{k-1} = t^k - \Delta t^{k-1}$, and the transformed boundary conditions $\mathbf{Z}$ at current time step.
2. Compute the coefficient matrices $\mathbf{A}(x_j)$ based on $\underline{\mathbf{C}}^k$, for all nodes, $j = 1, 2, \ldots, \text{TotNod}$.
3. If pure diffusion, i.e. $\mathbf{V} = \mathbf{0}$, go to Step 19.
4. Find and sort all eigenvalues λ_{ij} of each $\mathbf{A}(x_j)$, $i = 1, 2 \ldots, \text{Nos}$, $j = 1, 2, \ldots, \text{TotNod}$.
5. Compute eigenvectors χ_{ij} of each $\mathbf{A}(x_j)$, $i = 1, 2 \ldots, \text{Nos}$, $j = 1, 2, \ldots, \text{TotNod}$.
6. Find eigenmatrices $\mathbf{P}$ and $\mathbf{P}^{-1}$ for each $\mathbf{A}(x_j)$, $i = 1, 2 \ldots, \text{TodNod}$.
7. Transform $\underline{\mathbf{C}}^k$ and $\underline{\mathbf{C}}^{k-1}$ to $\underline{\mathbf{U}}^k$ and $\underline{\mathbf{U}}^{k-1}$, respectively.
8. Do Steps 9–11 for i from 1 to Nos.
9. Find the new position x'_j of each node at time level $t^{k+1} = t^k + \Delta t^k$ by forward tracking $x'_j = x_j + (v/n\lambda_{ij})\Delta t^k$
10. If x'_j is inside the domain of interest, interpolate the concentrations at x_j and restore them to $\underline{\mathbf{U}}^k$ according to

$$\underline{U}_i^{k+1}(x_j) = \text{Interpolate } \{\underline{U}_i^k(x'_j)\}$$

11. Else, compute the concentration according to boundary condition

$$\underline{\mathbf{U}}_i^{k+1}(x_j) = Z_i$$

12. Find $\underline{\tilde{\mathbf{C}}}_i^{k+1}$ from $\underline{\tilde{\mathbf{C}}}^{k+1} = \mathbf{P}\underline{\mathbf{U}}^{k+1}$
13. If pure advection, i.e. $\mathbf{D} = \mathbf{0}$, exit with $\underline{\tilde{\mathbf{C}}}_i^{k+1}$.
14. Do Steps 15–17 for i from 1 to Nos.
15. Find the original position x'_j of each node at time level $t^{k-1} = t^k - \Delta t^{k-1}$ by backward tracking

$$x'_j = x_j - \frac{v}{n\lambda_{ij}} \Delta t^{k-1}$$

16. If x'_j is inside the domain of interest, interpolate the concentrations at x_j and restore them to $\underline{\mathbf{U}}_i^{k-1}$ according to

$$\underline{U}_i^{k-1}(x_j) = \text{Interpolate } \{\underline{U}_i^{k-1}(x'_j)\}$$

17. Else, compute the concentration according to the boundary condition

$$\underline{\mathbf{U}}_i^{k-1}(x_j) = Z_i$$

18. Find $\underline{\tilde{\mathbf{C}}}_i^{k-1}$ from $\underline{\tilde{\mathbf{C}}}^{k-1} = \mathbf{P}\underline{\mathbf{U}}^{k-1}$
19. Compute global matrix $\mathbf{M}$ based on $\mathbf{A}$.
20. Update global vector $\mathbf{F}$ according to boundary conditions during $[t^k, t^k + \Delta t^k]$.
21. Compute a temporary matrix $\mathbf{R}^k$ according to

$$\mathbf{R} = \mathbf{M} - \frac{3\Delta t^k}{4}\mathbf{H}$$

22. Solve the concentration at time level $t^{k+1} = t^k + \Delta t^k$ according to

$$\underline{\mathbf{C}}^{k+1} = \mathbf{R}^{-1}\left(\mathbf{M}\underline{\tilde{\mathbf{C}}}^{k+1} - \frac{\Delta t^k}{4}\mathbf{H}\underline{\tilde{\mathbf{C}}}^{k-1} - \Delta t^k\mathbf{F}\right)$$

In the above pseudo-code, TotNod is the total number of nodes, subscript i is used for component i, subscript j is used for node j and superscript k is used for time level k. As there is no one best way to find the eigenvalues of a matrix, Step 4 in the above algorithm is left open. From the authors' experience, the shifted QR algorithm discussed, e.g. in Reference 13 is a remarkably simple method and works fine under very general circumstances. The eigenvalues must be sorted in the same order as the magnitudes of $\mathbf{A}$'s diagonal terms. For example, if A_{11} is the second biggest among all the diagonal terms, the corresponding eigenvalue λ_1 should also be the second biggest among all the eigenvalues.

A concern about the above algorithm is that there is no particular technique for handling a shock front that may be formed during the advection phase. As discussed by Sheng and Smith,[4] non-linear advection can create shock fronts and rarefaction areas in concentration. A shock front where characteristic lines carrying different concentrations meet may cause problems in particle tracking in Steps 9 and 15. For example, in Figure 1(a), the characteristic lines at nodes j and $j + 1$ meet during the time increment Δt^k and a shock front is formed between nodes $j + 1$ and $j + 2$ at time level t^{k+1}. After the formation of the shock front, the concentrations at nodes j and $j + 1$ are no longer carried along the original characteristic directions at the two nodes, but both along the shock front. Therefore, at the shock front the concentration steps from that at node j to that at node $j + 1$. Formation of a shock front depends on many factors like the initial and boundary conditions, number of components and the non-linearities involved. It is difficult to develop an algorithm for locating shock fronts for general purpose. A simple way of avoiding any shock front is to restrain the size of time step so that the new co-ordinates generated from the forward and backward tracking in Steps 9 and 15 satisfy

$$x'_{j+1} > x'_j \tag{28}$$

where x'_{j+1} is the downstream node and x'_{j+1} is the upstream node. This criterion for shock front control can be easily incorporated after Steps 9 and 15.

In the case where two characteristic lines separate from each other and a rarefaction area forms, the concentrations in the rarefaction area can be approximated by interpolation, as shown in Figure 1(b).

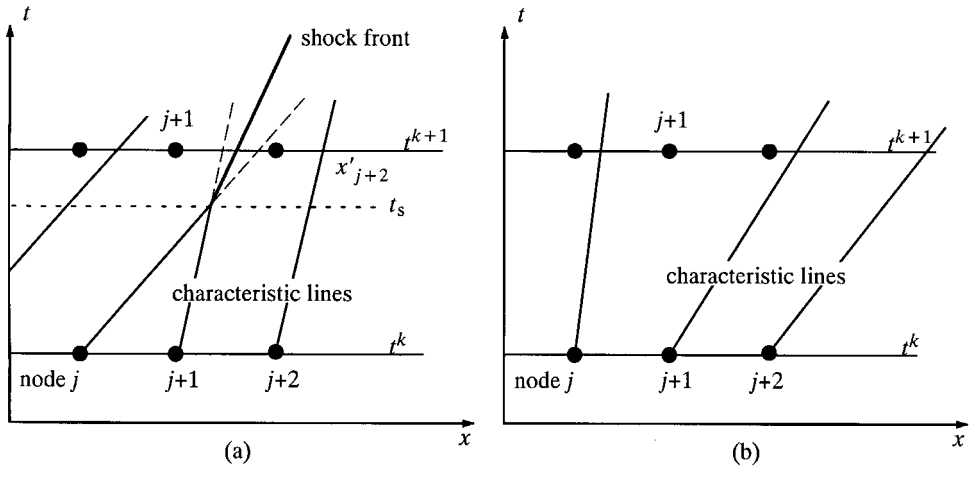

Figure 1. Characteristic lines cause formation of shock front (a) and rarefaction (b)

TRANSPORT–EQUILIBRIUM METHOD

An alternative technique for solving the transport problem of competitive components with Langmuir adsorption is to solve the transport equation (2) and the equilibrium equation (1) separately. In order to void the coupling effect in the transport equations, the liquid concentration C_i and the adsorbed concentration S_i on the left-hand side of equation (2) are replaced by the total concentrations T_i. Given liquid concentration C_i, the transport equation (2) can first be solved for the total concentrations T_i. The distributions of the total concentration in liquid and solid phases are then found by solving the equilibrium equation (1) where no time is involved. This process often involves iterations as the liquid concentration C_i is not known initially. In this paper, such a method is termed as the transport–equilibrium method and an example is presented here for the sake of comparison.

The transport–equilibrium method starts with the reformulation of the governing equation in terms of total concentrations including that in the liquid solution and that adsorbed on the solid surfaces:[5]

$$\frac{\partial T_i}{\partial t} = D_i \frac{\partial^2 C_i}{\partial x^2} - \frac{v}{n}\frac{\partial C_i}{\partial x} - E_i, \quad i = 1, 2 \ldots, \text{Nos} \tag{29}$$

where

$$T_i = C_i + \frac{\rho_d}{n} S_i$$

Equation (29) is a set of uncoupled partial differential equations and strictly speaking can not be solved as both T_i or C_i unknowns. However, in searching for an approximate solution time step by time step, the unknown concentration T_i at time level $t^{k+1} = t^k + \Delta t^k$ can be found given concentrations T_i and C_i at time level t^k. To illustrate this, we discretize T_i and C_i in the same way

as equation (23) and assume that the following discrete ordinary differential equations can somehow be generated from the governing equation (29) and boundary conditions:

$$\mathbf{M}\frac{\mathrm{D}\underline{\mathbf{T}}}{\mathrm{D}t} + \mathbf{H}\underline{\mathbf{C}} + \mathbf{F} = \mathbf{0} \tag{30}$$

where vectors $\underline{\mathbf{T}}$ and $\underline{\mathbf{C}}$ contain all nodal values of total and liquid concentrations, respectively, $\mathbf{M}$ and $\mathbf{H}$ are coefficient matrices, and $\mathbf{F}$ is a column vector:

Using a general θ method for time stepping, equation (30) can be approximated as

$$\mathbf{M}\frac{\underline{\mathbf{T}}^{k+1} - \underline{\mathbf{T}}^{k}}{\Delta t} + \mathbf{H}[(1-\theta)\underline{\mathbf{C}}^{k} + \theta\underline{\mathbf{C}}^{k+1}] + \mathbf{F}^{k+1} = \mathbf{0} \tag{31}$$

As both vectors $\mathbf{T}^{k+1}$ and $\mathbf{C}^{k+1}$ are unknown, equation (31) is in general not solvable. However, in the special case when $\theta = 0$, i.e. the forward Euler method, the only unknown vector is $\mathbf{T}^{k+1}$ and can be solved readily. Once $\mathbf{T}^{k+1}$ is known, the liquid concentration $\mathbf{C}^{k+1}$ and adsorbed concentration $\mathbf{S}^{k+1}$ can be found by solving the following system of equilibrium equations:

$$\underline{\mathbf{C}}^{k+1} + \frac{\rho_{\mathrm{d}}}{n}\underline{\mathbf{S}}^{k+1} = \underline{\mathbf{T}}^{k+1} \tag{32}$$

$$\underline{S}_i^{k+1} = \frac{K_i \underline{C}_i^{k+1} Q}{1 + \sum_{j=1}^{\mathrm{Nos}} K_j \underline{C}_j^{k+1}}, \quad i = 1, 2 \ldots, \mathrm{Nos} \tag{33}$$

where the underline stands for nodal values of the variables.

For an implicit time-stepping scheme with $\theta > 0$, the liquid concentration $\mathbf{C}^{k+1}$ found from the equilibrium equations has to be substituted into equation (31), resulting in $\underline{\mathbf{T}}^{k+1}$ of iteration two. Substituting this new $\underline{\mathbf{T}}^{k+1}$ into the equilibrium equations leads to the updated $\underline{\mathbf{C}}^{k+1}$ and $\underline{\mathbf{S}}^{k+1}$. The process is repeated until the difference in $\underline{\mathbf{T}}^{k+1}$ between two successive iterations converges to a specified tolerance.

One remaining issue for the transport–equilibrium method is to how to generate the ordinary differential equation system (30) from the partial differential equation system (29). Due to the ambiguity of the material derivatives in the mixed form (29), a Lagrangian formulation of the problem, as done for the characteristic finite element method described in the previous section, would not be easily possible. Therefore, a Eulerian approach has to be used to solve the advection–diffusion problem. The Petrov–Galerkin weighting procedure, which has been used successfully for solving independent advection–diffusion equations,[11] can be used here. In such a weighting procedure, the weighting functions are computed according to the so-called streamline upwind weighting

$$W_j = N_j + \xi \bar{W}_j = N_j + \xi \frac{\bar{l}}{2}\frac{\partial N_j}{\partial x}, \quad j = 1, 2, \ldots, \mathrm{Nod} \tag{34}$$

where ξ is a parameter between 0 and 1, and $\bar{l}$ is the characteristic length and in the one-dimensional case $\bar{l}$ is the length of the element. Setting $\xi = 0$ in the above equation leads to the standard Galerkin procedure and setting $\xi = 1$ leads to the full upwind weighting. Setting ξ according to

$$\xi = \coth(Pe) - \frac{1}{Pe} \tag{35}$$

leads to the optimal weighting.[11] The parameter Pe in equation (35) is the Peclet number defined as

$$Pe = \frac{v}{nD_{\min}} \frac{\bar{l}}{2} \tag{36}$$

where $D_{\min}$ the minimum diffusion coefficient of D_i, $i = 1, 2, \ldots, \text{Nos}$. This minimum value is used here in order to avoid different Peclet numbers for different components.

Applying the Petrov–Galerkin weighting procedure to equation (29) eventually leads to equation (30), with the coefficient matrices and vector defined as follows:

$$\mathbf{M} = \sum \int_{\Omega^e} \mathbf{W}^{\mathrm{T}} \mathbf{N} \, \mathrm{d}x \tag{37}$$

$$\mathbf{H} = \sum \int_{\Omega^e} \frac{\partial \mathbf{W}^{\mathrm{T}}}{\partial x} \mathbf{D} \frac{\partial \mathbf{N}}{\partial x} \, \mathrm{d}x + \sum \int_{\Omega^e} \mathbf{W}^{\mathrm{T}} \frac{v}{n} \frac{\partial \mathbf{N}}{\partial x} \, \mathrm{d}x \tag{38}$$

$$\mathbf{F} = \sum \int_{\Omega^e} \mathbf{W}^{\mathrm{T}} \mathbf{E} \, \mathrm{d}x + (\mathbf{W}^{\mathrm{T}} \mathbf{Q})|_{x=\Gamma_2} \tag{39}$$

In the equations above, $\mathbf{N}$ is the shape function matrix defined in equation (23), $\mathbf{W}$ is a matrix consisting of weighting functions and has a dimension of $\text{Nos} \times (\text{Nos} \times \text{Nod})$, $\mathbf{D}$ is a $\text{Nos} \times \text{Nos}$ diagonal matrix with D_i as its diagonal terms, and $\mathbf{E}$ is a $\text{Nos} \times \text{Nos}$ diagonal matrix with E_i as its diagonal terms. In equation (39), $\mathbf{E}$ is assumed to be concentration independent. For a concentration-dependent $\mathbf{E}$ such as the first-order kinetics, the $\mathbf{E}$ term contributes to matrix $\mathbf{H}$ in equation (38).[6] If the weighting function matrix $\mathbf{W}$ is set to the shape function matrix $\mathbf{N}$, the standard Galerkin weighting procedure is recovered.

The transport–equilibrium method described above can now be summarized in the following simplified pseudo-code.

1. Enter the minimum diffusion coefficient $D_{\min}$
2. Do Steps 3–7 for each element
3. Compute the Peclet number and the upwind parameter ξ of the element

   $$Pe = \frac{v}{nD_{\min}} \frac{\bar{l}}{2}$$

   $$\xi = \coth(Pe) - \frac{1}{Pe}$$
4. Compute the shape function N_j and its derivative $\partial N_j / \partial x$ for each node of the element, $j = 1, 2 \ldots, \text{Nod}$.
5. Compute the weighting function W_j and its derivative $\partial W_j / \partial x$ for each node of the element, $j = 1, 2 \ldots, \text{Nod}$.
6. Compute the element matrices and vectors $\mathbf{m}^e$, $\mathbf{h}^e$, and $\mathbf{f}^e$.
7. Assemble the element matrices to the global matrices $\mathbf{M}$, $\mathbf{H}$ and $\mathbf{F}$.
8. Enter the initial liquid concentrations $\underline{\mathbf{C}}^0$ and the iteration tolerance CTOL.
9. Compute the initial solid concentrations $\underline{\mathbf{S}}^0$ according to the equilibrium equation (33).
10. Compute the initial total concentration $\underline{\mathbf{T}}^0 = \underline{\mathbf{C}}^0 + \underline{\mathbf{S}}^0$
11. Set $k = 0$ and $t = 0$.
12. While $t < t_{\mathrm{f}}$, do Steps 13–21.

13. Enter the time increment Δt^k for the current step.
14. Update global vector $\mathbf{F}$ according to boundary conditions during $[t^k, t^k + \Delta t^k]$
15. Set $\underline{\mathbf{C}}^{k+1} = \mathbf{0}$, $\underline{\mathbf{T}}_1^{k+1} = \mathbf{0}$.
16. Solve the total concentration $\underline{\mathbf{T}}_2^{k+1}$ according to

$$\underline{\mathbf{T}}_2^{k+1} = \mathbf{M}^{-1}(\mathbf{M}\underline{\mathbf{T}}^k - (1-\theta)\Delta t^k \mathbf{H}\underline{\mathbf{C}}^k - \theta \Delta t^k \mathbf{H}\underline{\mathbf{C}}^{k+1} - \Delta t^k \mathbf{F})$$

17. Solve the equilibrium for $\underline{\mathbf{C}}^{k+1}$ and $\underline{\mathbf{S}}^{k+1}$.
18. Compute the norm

$$T_{\text{norm}} = \frac{\|\underline{\mathbf{T}}_2^{k+1} - \underline{\mathbf{T}}_1^{k+1}\|}{\|\underline{\mathbf{T}}_2^{k+1}\|}$$

19. If $T_{\text{norm}} \leqslant \text{CTOL}$, go to Step 21.
20. Else, set $\underline{\mathbf{T}}_1^{k+1} = \underline{\mathbf{C}}_2^{k+1}$ and go to Step 16.
21. Set $t = t + \Delta t^k$, $k = k + 1$

In the pseudo-code above, t_f is the final time of interest. As the equilibrium equations (32) and (33) are non-linear, iterative numerical solutions are in general sought in Step 17. However, for problems involving only one or two components, analytical solutions are possible.

The explicit form of he transport-equilibrium Petrov–Galerkin algorithm described above, i.e. without the iteration control in Steps 18–20, requires a similar amount of computational work as the characteristic finite element algorithm presented in the previous section. This explicit transport–equilibrium algorithm requires the solution of a system of non-linear equations, while the characteristic finite element algorithm requires the solution of the eigenvalues of a matrix of the same dimension. However, implicit forms of the transport–equilibrium Petrov–Galerkin algorithm require iterations between transport and equilibrium equations and hence are expected to be computationally less efficient. The actual performances of the two algorithms will be compared in the following section.

APPLICATION

The characteristic finite element (CFE) method and the tansport–equilibrium Petrov–Galerkin (TEPG) method are compared in terms of accuracy, stability and efficiency through a number of advection–diffusion problems in this section. The accuracy is checked by comparing the numerical results with exact solutions where available, or with reference solutions obtained using accurate numerical methods. The stability is measured by the smoothness and the time step dependence of the numerical results, as well as the conference of the methods. The efficiency is measured by the CPU time that an analysis uses.

The TEPG method actually includes a group of different methods, dependent on the time-stepping parameter θ. In this paper, three values of θ are studied, i.e. $\theta = 0$, 0·5 and 1. For adsorptive components with a non-linear adsorption isotherm, the TEPG methods with $\theta = 0{\cdot}5$ and 1 require iterations between the transport and equilibrium equations. The concentration tolerance CTOL used to control the conference of the TEPG methods is set to 10^{-4}. In addition, the maximum number of iterations during each time step is limited to 100. If no convergence is achieved within the maximum iterations, the analysis is regarded as a failure.

Table I. Material properties for Example 1: advection–diffusion of a non-adsorptive component

Cases	n	ρ	v	D	Pe	Transport
I	0·5	1·5	1	0	∞	Pure advection
II	0·5	1·5	1	0·1	1	Advection–diffusion
III	0·5	1·5	0	0·1	0	Pure diffusion

The dimensionless Courant number Cr is used to indicate the effects of time step on the numerical results. This parameter is defined as

$$Cr = \begin{cases} \dfrac{v}{n}\dfrac{\Delta t}{h}, & v > 0 \\ D\dfrac{\Delta t}{h^2}, & v = 0 \end{cases} \tag{40}$$

where h is the element length.

The CPU times used in this section are all for a Pentium Pro 200 MHz processor with a Borland C++ compiler 4·02. Each of these times is further divided by the number of time steps used in the analysis.

The problems considered in this section all deal with advection and diffusion of chemical components in a soil column. The length of the soil column is 10 units. The material properties shared in all the examples are given in Table I. Three different cases, representing a pure advection, a combined advection–diffusion and a pure diffusion problem, respectively, are considered for each problem. The velocity is positive in the direction of increasing x. The soil column is divided into 100 equal linear elements. The Peclet numbers in Table I are for one single element.

Advection and diffusion of non-adsorptive components

As the first example, advection and diffusion of non-adsorptive components in the soil column is considered. Since no chemical equilibrium equation is involved, concentrations of different components can be solved independently and we need only to demonstrate the solutions for one component.

The initial concentration in the soil column is set to zero. A unit concentration is continuously injected at the inflow end of the soil column, i.e. $C(x = 0, t) = 1$. For Cases I and II where $v > 0$, no outflow boundary condition at $x = 10$ is need. For Case III, the concentration at the outflow boundary is diluted to 0, i.e. $C(x = 10, t) = 0$.

For this simple example, the total concentration equals the liquid concentration at each node. Since no iteration is needed, the TEPG method reduces to the Petrov–Galerkin method. The time-stepping scheme in Step 16 in the TEPG algorithm can be formulated in a slightly different way to avoid iteration

$$\underline{\mathbf{C}}_2^{k+1} = (\mathbf{M} + \theta\,\mathrm{d}t\mathbf{H})^{-1}(\mathbf{M}\underline{\mathbf{C}}^k - (1-\theta)\Delta t^k\mathbf{H}\underline{\mathbf{C}}^k - \Delta t^k\mathbf{F}) \tag{41}$$

Analytical solutions exist for all the three cases. In Case I, the exact solution of the pure advection problem is simply a translation of the initial concentration according to

$$C(x, t) = C^0\left(x - \frac{v}{n}t\right) \tag{42}$$

In Cases II and III, the exact solutions are given as

$$C(x, t) = \frac{1}{2}\operatorname{erfc}\left(\frac{x - (v/n)t}{\sqrt{4Dt}}\right) + \frac{1}{2}\exp\left(\frac{vx}{nD}\right)\operatorname{erfc}\left(\frac{x + (v/n)t}{\sqrt{4Dt}}\right) \tag{43}$$

The numerical results are compared with these analytical solutions in Figure 2. In Case I where advection is the only transport mechanism, the CFE method gives exact nodal concentrations both for $Cr = 1$ and 2. The TEPG method with $\theta = 0$ also predicts exact nodal concentrations for $Cr = 1$, but gives purely oscillatory results for $Cr = 2$. The TEPG methods with $\theta = 0{\cdot}5$ and 1 are stable, but both introduce numerical 'diffusion' at the concentration front. This numerical 'diffusion' increases with increasing θ or increasing Courant number. In Case II where both advection and diffusion take place, the CFE method gives very accurate results both for $Cr = 1$ and 2. The TEPG method with $\theta = 0{\cdot}5$ is also accurate and the results are only marginally different from those of the CFE method. The TEPG method with $\theta = 1$ is stable, but overestimates the diffusion effect. This overestimation is more pronounced for $Cr = 2{\cdot}0$. The TEPG method with $\theta = 0$ is not stable for $Cr = 1$ or 2. In case III where only diffusion occurs, the CFE method and the two TEPG methods with $\theta = 0{\cdot}5$ and 1 are all accurate and the results are only marginally different from the exact solution. The TEPG method with $\theta = 0$ again gives purely oscillatory results for $Cr = 1$ or 2.

In terms of efficiency, the three TEPG methods use the same amounts of CPU time for each case. The average CPU time per time step required by the TEPG methods in Case I is identical to that in Case II, but 80 per cent more than that in Case III. The CFE method requires only 3 per cent CPU time of he TEPG methods for Case I, but required 33 and 10 per cent more CPU times for Cases II and III, respectively.

The results for this example indicate that the CFE method is very accurate for advection–diffusion problems where the Peclet number varies from zero to infinite. It has also been confirmed that the TEPG method with $\theta = 0$ is generally not stable. This method will not be used in the following examples.

Advection of single adsorptive component

For a single component, the Langmuir adsorption isotherm takes the form

$$S = \frac{KCQ}{1 + KC} \tag{44}$$

where K is set to 1 and Q is set to $0{\cdot}5$ in this example. The properties for the soil column as well as the initial and boundary conditions are kept the same as in the previous example. To start with, we first consider the pure advection problem, i.e. Case I in Table I. Problems involving diffusion will be considered in the following example.

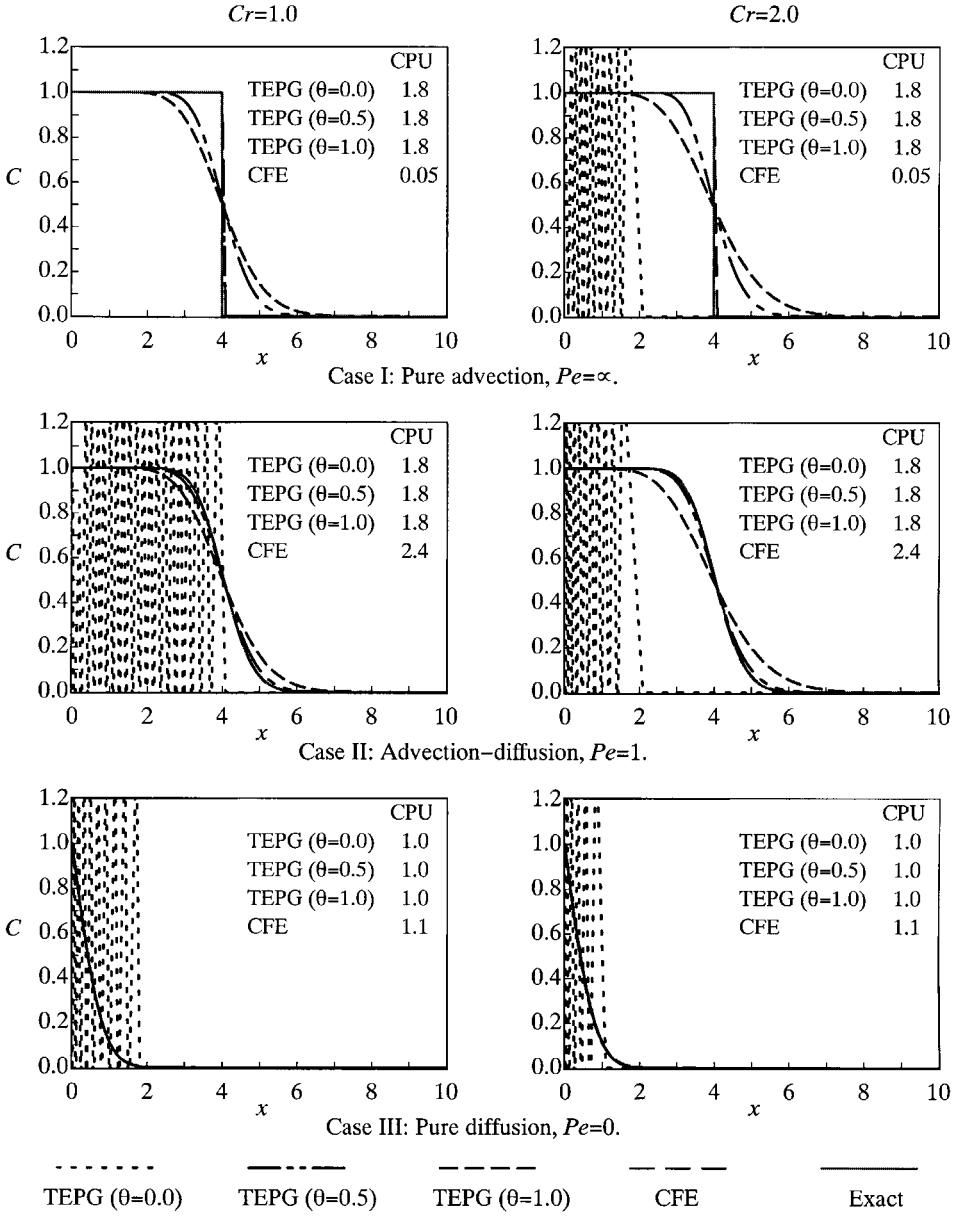

Figure 2. Advection and diffusion of a non-adsorptive component, concentrations at $t = 2$

Analytical solutions to advective transport of adsorptive components were given by Sheng and Smith.[4] For a soil column with a continuous injection of a constant concentration t one of its ends, the analytical solution is

$$C(x, t) = C^0(x - v_c t) \tag{45}$$

where C^0 is the initial concentration distribution, and v_c is the transport velocity at concentration C given by

$$v_c = \frac{v}{n + \rho_d QK/(1 + KC)^2} \tag{46}$$

The initial concentration distribution in this example is zero everywhere except at $x = 0$ where $C^0 = 1$. Therefore, there is initially a concentration discontinuity at $x = 0$. As the material particles on its upstream side ($x = 0^-$) travel faster than those on its downstream side ($x = 0^+$), this concentration discontinuity forms a shock front immediately for $t \geqslant 0$. The velocity of the shock front is[4]

$$v_s = \frac{v}{n + \rho_d QK/(1 + KC_u)(1 + KC_d)} \tag{47}$$

where C_u and C_d are the concentration at the upstream and downstream side of the shock front, respectively. In this example,

$$C_u = C^0(x = 0^-) = 1 \tag{48}$$

$$C_d = C^0(x = 0^+) = 0 \tag{49}$$

Inserting these values into equation (47) gives the shock front velocity $v_s = 1{\cdot}14$. This is compared to the transport velocities

$$\frac{v}{n} = 2{\cdot}0 \quad \text{for non-adsorptive component}$$

$$v_c(C = 1) = \frac{v}{n + \rho_d QK/(1 + KC)^2} = 1{\cdot}45 \quad \text{for adsorptive component at } C = 1$$

$$v_c(C = 0) = \frac{v}{n + \rho_d QK/(1 + KC)^2} = 0{\cdot}8 \quad \text{for adsorptive component at } C \to 0$$

The velocity $v_c\,(C = 0)$ also equals the transport velocity when a linear adsorption isotherm based on the initial tangent of the Langmuir isotherm is used. It can be seen that the shock front velocity is retarded by 57 per cent from the non-adsorptive velocity, but increased by 43 per cent from the transport velocity using the linear adsorption isotherm. As the concentrations are uniform on both the downstream and upstream sides of the shock front, the exact solution of concentration distribution at any time can be expressed by equation (45) with v_c replaced by v_s.

Either of the two numerical methods described in this paper deals with formation of shock fronts explicitly. As pointed out before, the current strategy to avoid shock fronts in the CFE method is to limit the time step so that an upstream particle will not travel across a downstream particle. For this example, the limit on the time step is

$$\Delta t < \frac{h}{v(C = 10) - v(C = 0)} = \frac{0{\cdot}1}{1{\cdot}45 - 0{\cdot}8} = 0{\cdot}154$$

This means that the Courant number in equation (40) must be less than 3·08. Taking into account the shock front velocity, we use two Courant numbers 0·5 and 1·0 for this example.

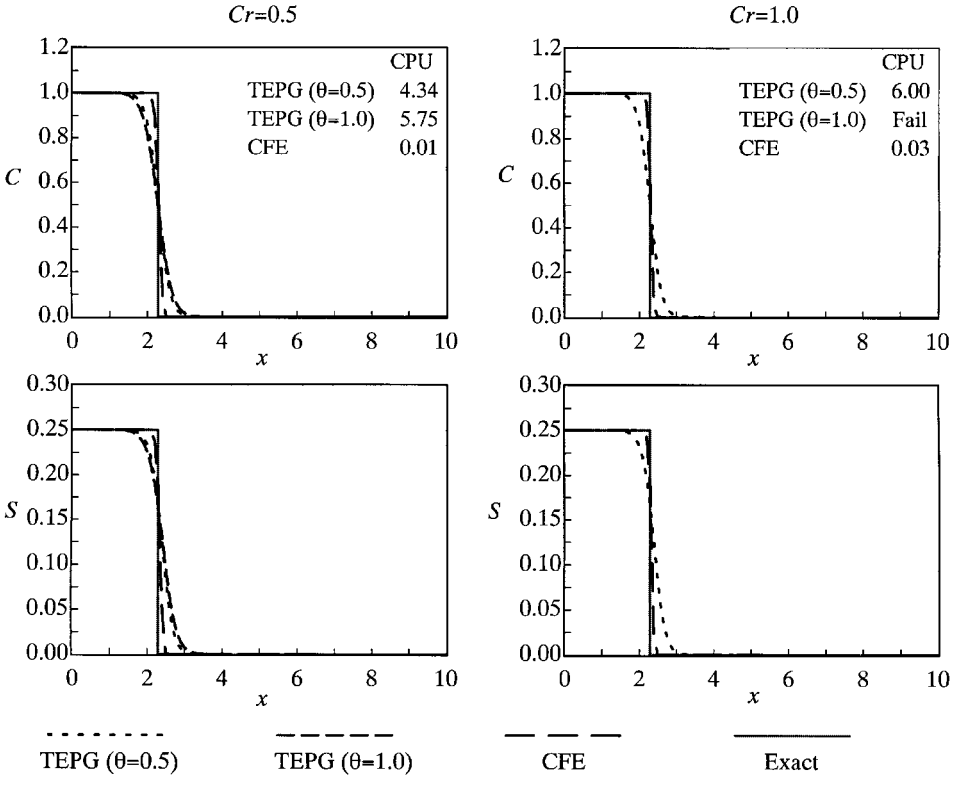

Figure 3. Advection of an adsorptive component, $Pe = \alpha \propto$, concentrations at $t = 2$

The numerical results for this example are presented in Figure 3. The TEPG method $\theta = 0$ gives purely oscillatory results and is excluded here. In both cases $Cr = 0{\cdot}5$ and 1·0, the CFE method gives very accurate results and the numerical 'diffusion' at the concentration front are not pronounced. The TEPG methods with $\theta = 0{\cdot}5$ and 1 both introduce numerical 'diffusion' near the concentration front. In the case $Cr = 0{\cdot}5$, the TEPG method with $\theta = 1$ gives the least accurate results. In the case $Cr = 1{\cdot}0$, the TEPG method with $\theta = 1$ fails in convergence in the transport–equilibrium iteration.

In terms of CPU time, the CFE method is significantly faster than the TEPG methods. The CFE method typically uses 0·3 per cent CPU time of the TEPG methods for this advection problem. In the case of $Cr = 0{\cdot}5$, the TEPG method with $\theta = 0{\cdot}5$ uses 75 per cent CPU time of the TEPG method $\theta = 1$.

The results obtained from this example show that the CFE method is more accurate and significantly faster than the TEPG methods for the advection problem with a non-linear adsorption isotherm. The CFE method predicts accurately the shock front velocity. The TEPG method with $\theta = 0{\cdot}5$ also approximates well the shock front location, but gives more pronounced numerical 'diffusion'. The TEPG method with $\theta = 1$ is found to be not convergent for a large time step.

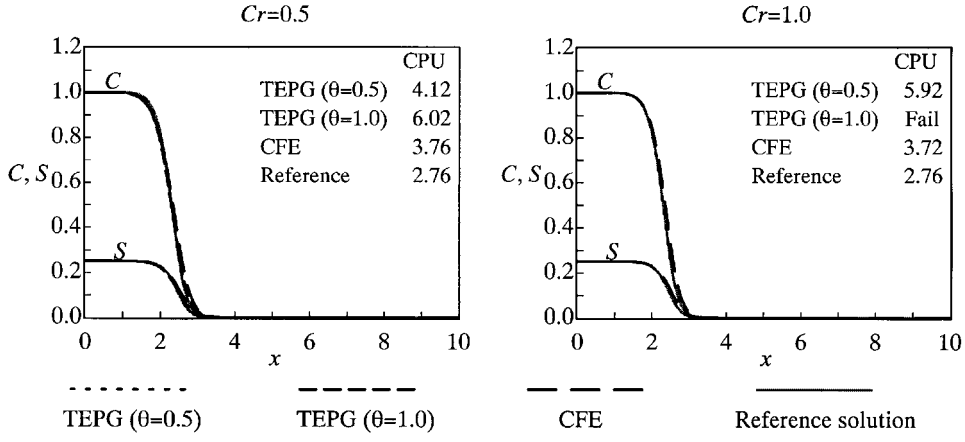

Figure 4. Advection and diffusion of an adsorptive component, $Pe = 1$, concentrations at $t = 2$

Advection and diffusion of a single adsorptive component

No analytical solution is currently available for the cases when diffusion is also involved. In order to check the accuracy of numerical results, we use a very small time step ($Cr = 0{\cdot}01$) to obtain a reference check the accuracy of numerical results, we use a very small time step ($Cr = 0{\cdot}01$) to obtain a reference solution. With such a small Courant number, the CFE and TEPG methods give basically identical results, and in this example the TEPG method with $\theta = 0{\cdot}5$ is used to obtain the reference solution.

The numerical results for Cases II with non-linear adsorption are shown in Figure 4. For both $Cr = 0{\cdot}5$ and $1{\cdot}0$, the CFE method and the TEPG method with $\theta = 0{\cdot}5$ is used to obtain the reference solution.

The numerical results for Cases II with non-linear adsorption are shown in Figure 4. For both $Cr = 0{\cdot}5$ and $1{\cdot}0$, the CFE method and the TEPG method with $\theta = 0{\cdot}5$ are very accurate and their results are only marginally different from the reference solution. The TEPG method with $\theta = 1$ is also accurate for $Cr = 0{\cdot}5$, but fails to converge for $Cr = 1{\cdot}0$.

In terms of efficiently, the CFE method uses less CPU times than the two TEPG methods. The average CPU time per time step for the CFE method does not vary much as the Courant number increases. However, the TEPG methods require more CPU time per time step as the Courant number increases.

The numerical results for Case III, shown in Figure 5, follow the same observations for Case II, except that the TEPG method with $\theta = 1$ fails both for $Cr = 0{\cdot}5$ and $1{\cdot}0$ here. The average CPU time per time step used by the TEPG method with $\theta = 0{\cdot}5$ for this case increases more significantly with increasing Courant number than for Case II.

The results from this example show that the CFE method and the TEPG method with $\theta = 0{\cdot}5$ have the same accuracy for the advection–diffusion problem with a non-linear adsorption isotherm, with the former being more efficient for large time steps. The TEPG method with $\theta = 1$ has difficulties in convergence, especially for large time steps and for diffusion-dominant problems.

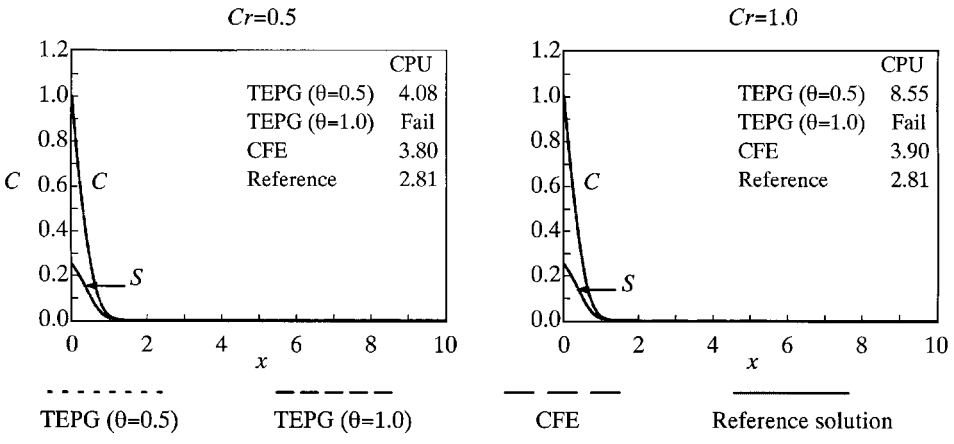

Figure 5. Diffusion of an adsorptive component, $Pe = 1$, concentrations at $t = 2$

Advection and diffusion of two competitive components

This example deals with advective–diffusive transport of two competitive components in the soil column. The properties of the two components are

$$K_1 = 1, \qquad C_1(0, t) = 1, \qquad C_1(x > 0, 0) = 0$$

$$K_2 = 10, \qquad C_2(0, t) = 1, \qquad C_2(x > 0, 0) = 0$$

The maximum adsorption capacity Q of the soil is set to 0·5. The soil porosity n is set to 0·5 and the dry density ρ to 1·5. Again three different cases are considered. In Case I, the Darcian fluid velocity v is set to 1 and the diffusion coefficients D_1 and D_2 are set to 0. In Case II, $v = 1$ and $D_1 = D_2 = 0{\cdot}1$. In case III, $v = 0$ and $D_1 = D_2 = 0{\cdot}1$. The downstream boundary concentrations at $x = 10$ are set to 0 in Case III.

With the help of mathematical theorems for systems of non-linear hyperbolic equations,[14] it is possible to illustrate the analytical solution for Case I. As it has a smaller adsorption parameter, component 1 is expected to travel faster than component 2. Two shock fronts are thus expected, one at the concentration front for component 1 and the other at the concentration front for component 2, i.e. x_1 and x_2 in Figure 6. Since no diffusion is involved in Case I, the concentrations behind the shock front x_2 in Figure 6. Since no diffusion is involved in Case I, the concentrations behind the shock front x_2, i.e. within $[0, x_2]$, are uniform and determined by the boundary condition at $x = 0$, i.e. $C_{1a} = C_2 = 1$, $S_{1a} = 0{\cdot}5/12$ and $S_2 = 5/12$. Between the two shock fronts $[x_2, x_1]$, the concentrations C_{1b} and S_{1b} are also uniform, if no rarefaction waves develop. The adsorbed concentration S_{1b} is expected to be larger than S_{1a}, due to the absence of the competition from component 2. The liquid concentration C_{1b} within $[x_2, x_1]$ is also expected to be larger than C_{1a}, due to the release of the adsorbed concentration S_1 from S_{1b} to S_{1a}. The competitive adsorption in this example has actually the same effects as ion exchange and desorption. The increase in the downstream concentration (larger than the injected concentration) due to ion exchange is often observed in laboratory tests and in field.[10,15]

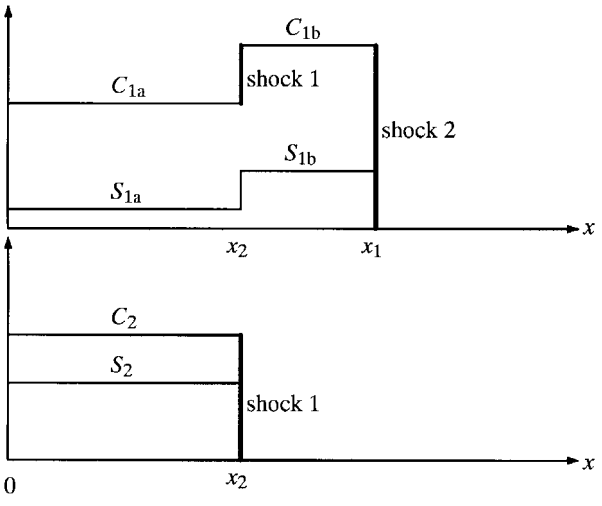

Figure 6. Advection of two competitive components (Case I)

In general, the increase of the total concentration of each component during time interval Δt in the soil column must equal the injected concentration at $x = 0$, i.e.

$$(nC_{1a} + \rho S_{1a})\,\mathrm{d}x_2 + (nC_{1b} + \rho S_{1b})(\mathrm{d}x_1 - \mathrm{d}x_2) = C_{1a} v\,\mathrm{d}t, \quad x_2 < x_1 \leqslant 10 \tag{50}$$

$$(nC_2 + \rho S_2)\,\mathrm{d}x_2 = C_2 v\,\mathrm{d}t, \quad x_2 < x_1 \leqslant 10 \tag{51}$$

where for this example $C_{1a} = C_2 = 1$, $v = 1$, $n = 0{\cdot}5$, $\rho = 1{\cdot}5$, $S_{1a} = 0{\cdot}5/12$ and $S_2 = 5/12$. The concentration S_{1b} is related to the concentration C_{1b} through equation (1). The velocity of the first shock front at x_1 is given by (47), i.e.

$$v_{s1} = \frac{\mathrm{d}x_1}{\mathrm{d}t} = \frac{v}{n + \rho Q K_1/(1 + K_1 C_{1b})} \tag{52}$$

There are four unknowns $v_{s1} = \mathrm{d}x_1/\mathrm{d}t$, $v_{s2} = \mathrm{d}x_2/\mathrm{d}t$, C_{1b}, and S_{1b}, and S_{1b} in four equations (1) and (50)–(52). Solving these equations yields

$$C_{1b} = 1{\cdot}65, \qquad S_{1b} = 0{\cdot}31, \qquad v_{s1} = \frac{\mathrm{d}x_1}{\mathrm{d}t} = 1{\cdot}28, \qquad v_{s2} = \frac{\mathrm{d}x_2}{\mathrm{d}t} = 0{\cdot}89$$

By comparing the upstream and downstream transport velocities, it is easy to prove that x_1 and x_2 are real shock fronts for components 1 and 2, respectively. With known C_{1b}, it is also possible to prove that x_2 is a real shock front, not a rarefaction shock, for component 1. This confirms the assumption made earlier. Due to space limitations, the proof will not be presented in this paper. The analytical solution given above can also be obtained from multicomponent chromatography, see e.g. Reference 16.

In Figure 7, the numerical results for Case I are compared with the known exact solution obtained above. As in the previous example, concentrations are plotted at time $t = 2$. The TEPG method with $\theta = 1$ fails in convergence both for $Cr = 0{\cdot}5$ and $1{\cdot}0$. In the case $Cr = 0{\cdot}5$, the CFE method gives relatively accurate results for concentrations, though numerical 'diffusion' is noticed

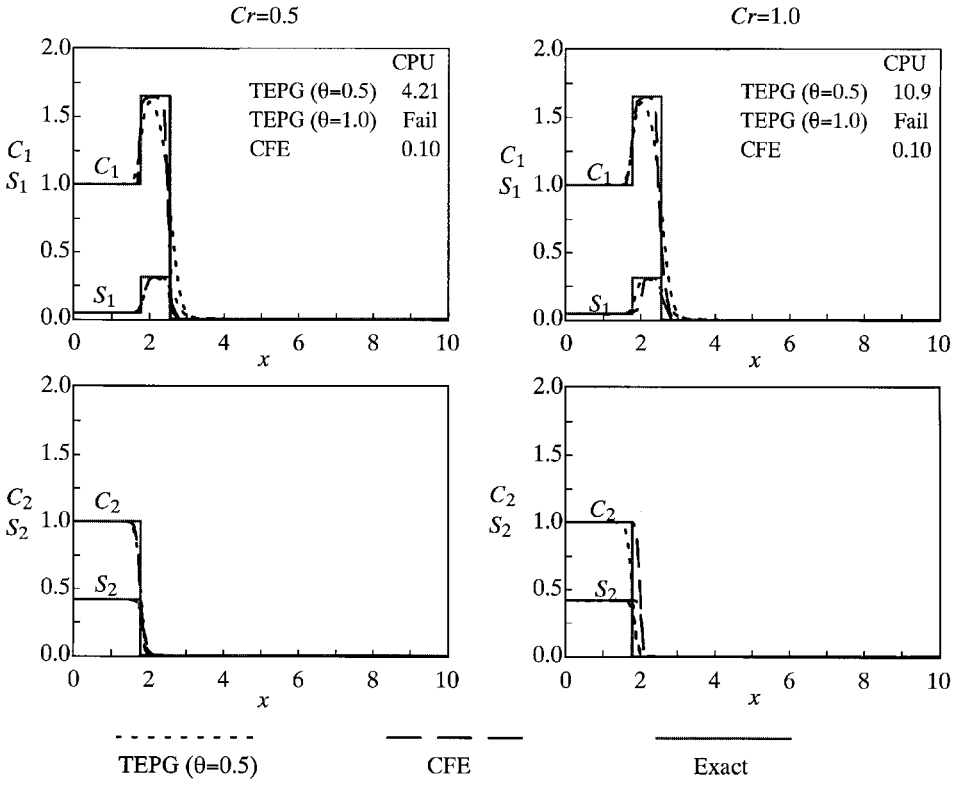

Figure 7. Advection of two competitive components, $Pe = \infty$, concentrations at $t = 2$

at the two shock fronts. The increase in the liquid and adsorbed concentrations of component 1 between the two shock fronts are well captured. The TEPG method with $\theta = 0{\cdot}5$ also gives good results, but with more pronounced numerical 'diffusion' than the CFE method. In the case $Cr = 1{\cdot}0$, the CFE method somewhat overestimates the velocity of the shock front x_2. The TEPG method with $\theta = 0{\cdot}5$ gives a slightly better prediction of the shock front location, but again gives more pronounced numerical 'diffusion'. In terms efficiency, the CFE method uses about 2 per cent for $Cr = 0{\cdot}5$ and 0·9 per cent for $Cr = 1$ CPU times of the TEPG method with $\theta = 0{\cdot}5$.

In Cases II and III, no analytical solution is available. The analytic solution for Case I is used as a reference solution. The numerical results at time $t = 2$ for Case II is shown in Figure 8. The TEPG method with $\theta = 1$ fails again in the both analyses for $Cr = 0{\cdot}5$ and 1·0. In the case for $Cr = 0{\cdot}5$, the CFE method and the TEPG method with $\theta = 0{\cdot}5$ are only marginally different. In the case for $Cr = 1{\cdot}0$, the CFE method gives a larger velocity of the shock front x_1 than the TEPG method with $\theta = 0{\cdot}5$. In terms of efficiency, the average CPU time required by CFE method per time step is only 95 per cent for $Cr = 0{\cdot}5$ and 47 per cent for $Cr = 1{\cdot}0$ of that by the TEPG method with $\theta = 0{\cdot}5$.

The concentrations predicted by the CFE method at time $t = 1$ and 4 for Case II are also presented here in Figure 9 for comparison. It can be seen that the peak concentration in C_1 at

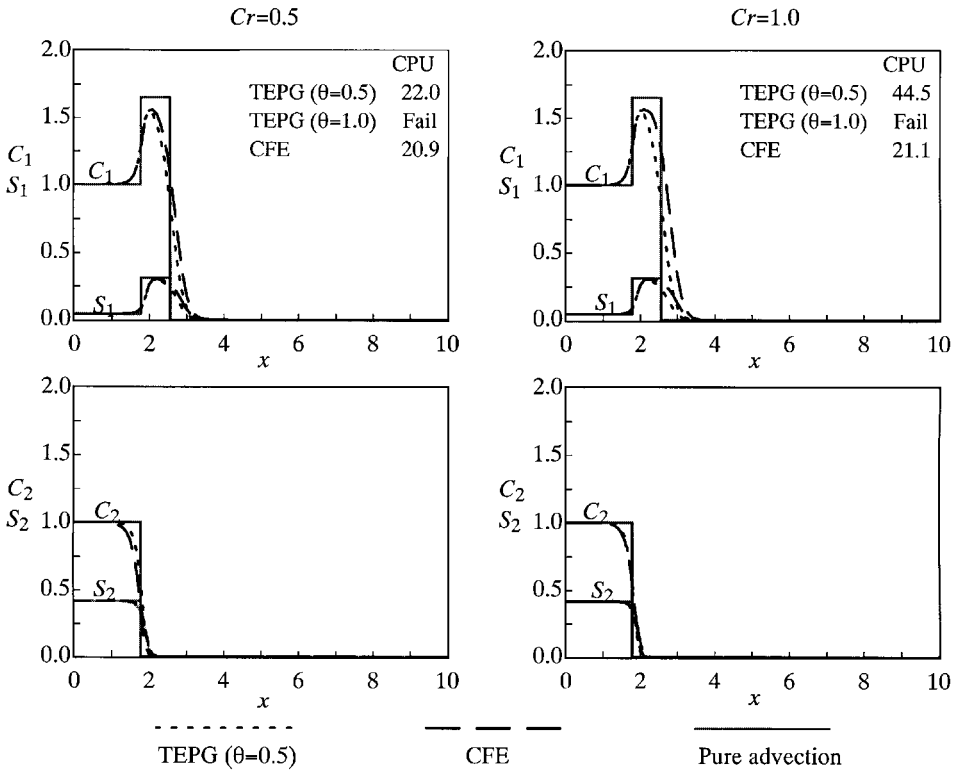

Figure 8. Advection and diffusion of two competitive components, $Pe = 1$, concentrations at $t = 2$

$t = 1$ is less than the exact solution 1·65 for pure advection, due to the effect of diffusion in Case II. The distance between the two concentration fronts increases with increasing time.

In Case III where diffusion is the only transport mechanism, no concentration increase in C_1 is observed. However, it can be seen that component 1 diffuses to a larger distance than component 2. An increase in the adsorbed concentration S_1 can also be observed. The numerical results from the CFE method and TEPG method with $\theta = 0{\cdot}5$ are almost identical (Figure 10). The TEPG method with $\theta = 0{\cdot}5$ fails to give a solution for the case $Cr = 1{\cdot}0$. The CPU time per time step used by the CFE method is about 76 per cent of that by the TEPG method with $\theta = 0{\cdot}5$.

CONCLUSION

The characteristic finite element method presented in this paper is found to be appropriate for solving advective–diffusive transport equations coupled with non-linear competitive adsorptive equations. The accuracy and efficiency of this method for advection-dominated problems are particularly advantageous. It captures well the shock front locations in non-linear advection problems. The transport-equilibrium Petrov–Galerkin method with a forward Euler time-stepping scheme, which avoids the iteration between the transport and equilibrium equations, is in

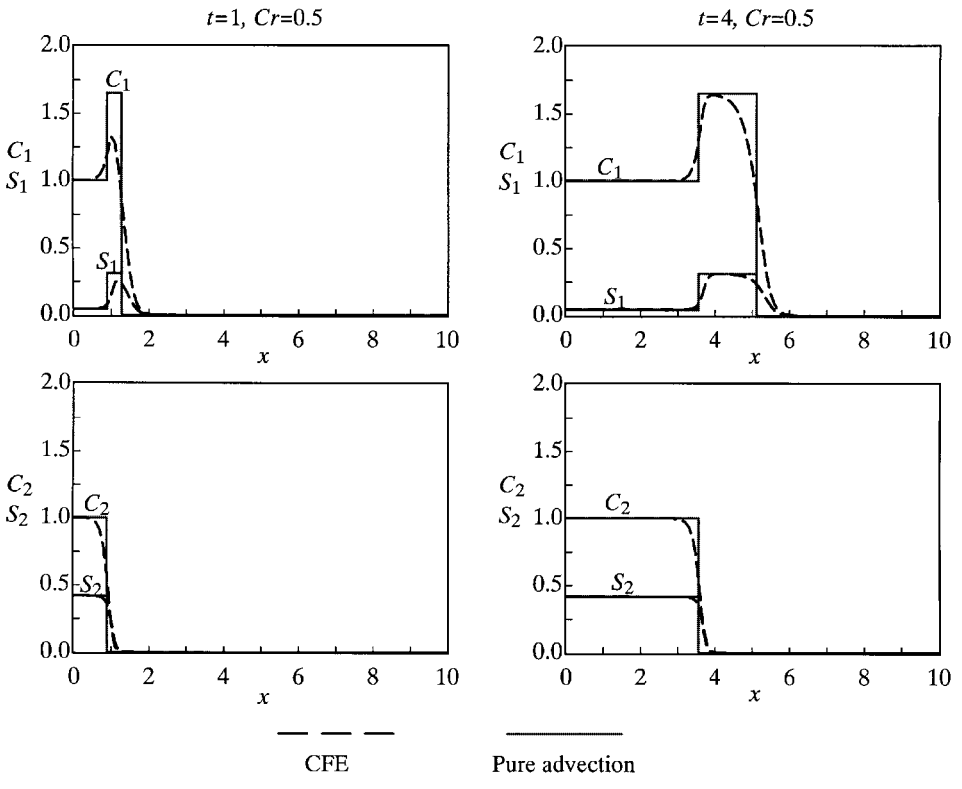

Figure 9. Advection and diffusion of two competitive components, predicted by the CFE method, $Pe = 1$, concentrations at $t = 1$ and 4

general not stable and may give purely oscillatory results. Therefore, this method cannot be recommended. The transport-equilibrium Petrov–Galerkin method with a middle point time-stepping scheme performs best among the three TEPG methods. This method is stable, convergent in most cases and gives accurate results for diffusion-dominated problems. It does introduce numerical 'diffusion' for advective problems. As it is easy to implement, this method can also be recommended. The transport–equilibrium Petrov–Galerkin method with a full backward Euler time-stepping scheme has difficulties in reaching convergence between the transport and equilibrium equations and hence cannot be recommended.

From a practical viewpoint, the numerical examples examined here have made it clear that with non-linear competitive adsorption isotherms in the transport equations, the contaminant transport process is significantly more complicated. For example, the downstream pore fluid and sorbed concentrations of a contaminant can be larger than its concentrations at the source. Such phenomena, while observed in laboratory and field, cannot be predicted using linear adsorption isotherm.

Although the focus of this paper was put on the non-linear Langmuir adsorption equation, the strategies in the algorithms presented should also be applicable to transport problems coupled with other types of non-linear equations.

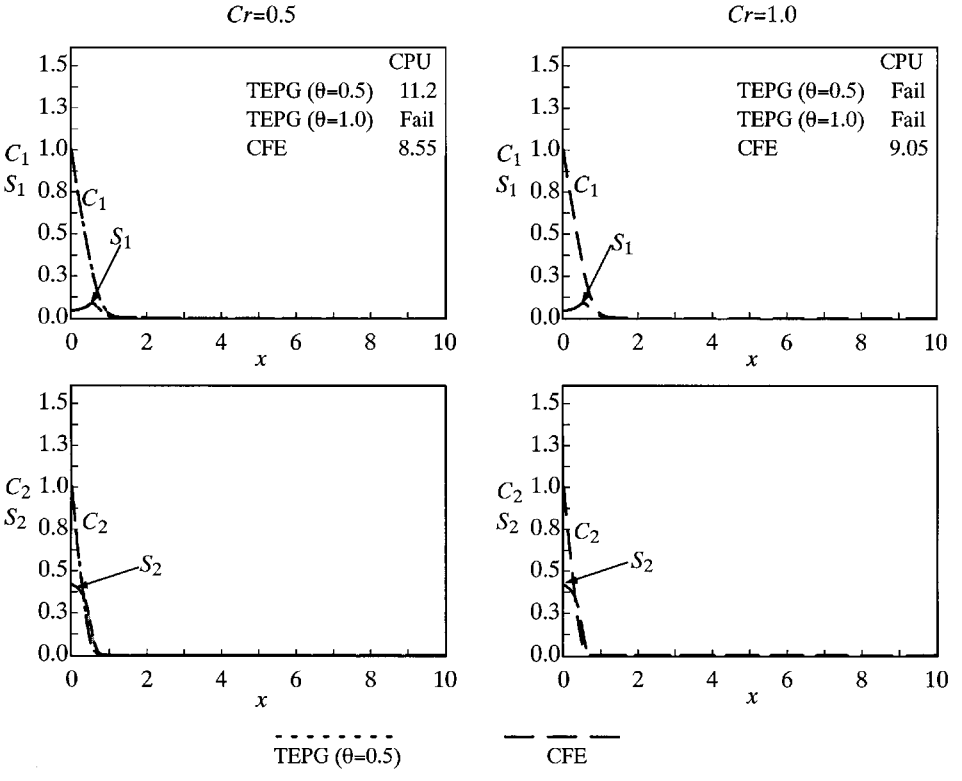

Figure 10. Diffusion of two competitive components, $Pe = 1$, concentrations at $t = 2$

REFERENCES

1. C. D. Shackelford and R. K. Rowe, 'Contaminant transport modelling', in P. S. Seco e Pinto (ed.), *Proc. 3rd Int. Congress on Environmental Geotechnics* Vol. 3, Balkema, Rotterdam, 1998, pp. 939–956.
2. V. Murali and L. A. Aylmore, 'Competitive adsorption during solute transport in soils: 1. mathematical models', *Soil Sci. Soc. Am. J.* **135**(3)**,** 143–150 (1983).
3. G. Sposito, *The Chemistry of Soils*, Oxford University Press, New York, 1989.
4. D. Sheng and D. W. Smith, 'Analytic solutions to the advective contaminant transport equation with nonlinear sorption', *Int. J. Numer. Anal. Meth. Geomech.* **23,** 853–879 (1999).
5. G. T. Yeh and V. S. Tripathi, 'A critical evaluation of recent developments in hydrogeochemical transport models of reactive multichemical components', *Water Resources Res.* **25**(1)**,** 93–108 (1989).
6. D. Sheng and K. Axelsson, 'Uncoupling of coupled flows in soil, a finite element method', *Int. J. Numer. Anal. Meth. Geomech.* **19,** 537–553 (1995).
7. R. D. Harter and D. E. Baker, 'Application and misapplications of the Langmuir equation to soil adsorption phenomena', *Soil Sci. Soc. Am. J.* **41,** 1077–1080 (1977).
8. A. W. Adamson, *Physical Chemistry of Surfaces*, 4th edn, Wiley, New York, 1982.
9. C. W. Jeong and K. J. Lee, 'Propagation of concentration waves through a sorption medium with simultaneous ion exchange and electrolyte adsorption', *Waste Management*, **12,** 61–73 (1992).
10. R. K. Rowe, R. W. Quigley and J. R. Booker, *Clayey Barrier Systems for Waste Disposal Facilities*, E and FN Spon (Chapman & Hall), London, England, 1995.
11. O. C. Zienkiewicz and R. L. Taylor, *The Finite Element Method*, 4th edn, Vol. 2, McGraw-Hill, London, 1991.

12. D. Sheng, K. Axelsson and S. Knutsson, 'Finite element analysis for convective heat diffusion with phase change', *Compu. Meth. Appl. Mech. Engng.* **104**(1)**,** 19–30 (1993).
13. G. Strang, *Linear Algebra and its Applications*, 3rd edn, Harcout Brace Jovanovich, San Diego, 1988.
14. R. Courant and D. Hilbert, *Method of Mathematical Physics*, Vol. II, Wiley-Interscience, New York, 1962.
15. J. T. Dance and E. J. Reardon, 'Migration of contaminants in groundwater at a landfill: a case study', *J. Hydrol.* **63,** 109–130 (1983).
16. F. Helfferich and G. Klein, *Multicomponent Chromatography*, *Theory of Interference*, Marcel Dekker, New York, 1970.

